

**Supplementary Materials for
Tunable valley splitting and magnetic anisotropy in two-dimensional
buckled honeycomb lattice Mn_2X_2 ($\text{X} = \text{F}, \text{Cl}, \text{Br}$)**

Mingyu Lü¹, Wendan Song¹, Yuping Tian¹, Chao-Bo Wang¹, Xuefeng Dai,¹ Xudong Su¹, Xiangru Kong^{1,*},
Wei-Jiang Gong^{1,*}

¹College of Sciences, Northeastern University, Shenyang 110819, China

*Corresponding authors: kongxiangru@mail.neu.edu.cn and gwj@mail.neu.edu.cn

TABLE S1: Calculated optimized lattice constants (a), nearest Mn–Mn distances (d), Mn–X–Mn angles (α), cohesive energy (ΔE_{coh}), and the energy differences of the FM and AFM2 states with respect to the AFM1 state (meV/unit cell).

<i>Material</i>	a (Å)	d (Å)	α (°)	ΔE_{coh} (eV/atom)	$\Delta E_{\text{FM-AFM1}}$	$\Delta E_{\text{AFM2-AFM1}}$
Mn ₂ F ₂	3.07	2.64	91.7	-4.180	374.972	281.069
Mn ₂ Cl ₂	3.37	2.66	84.9	-3.297	583.703	480.695
Mn ₂ Br ₂	3.54	2.69	84.0	-2.957	621.503	536.694

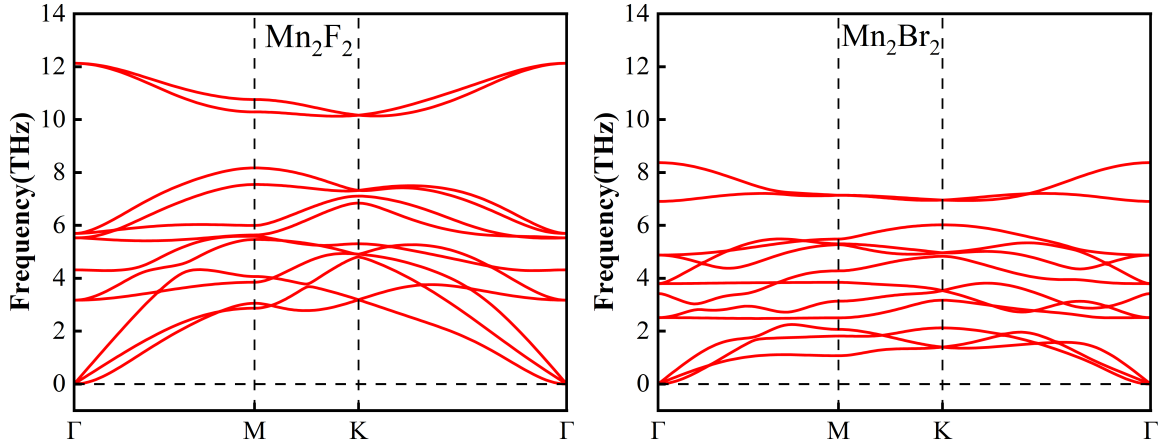


FIG. S1: Phonon spectra of Mn₂Br₂ and Mn₂F₂.

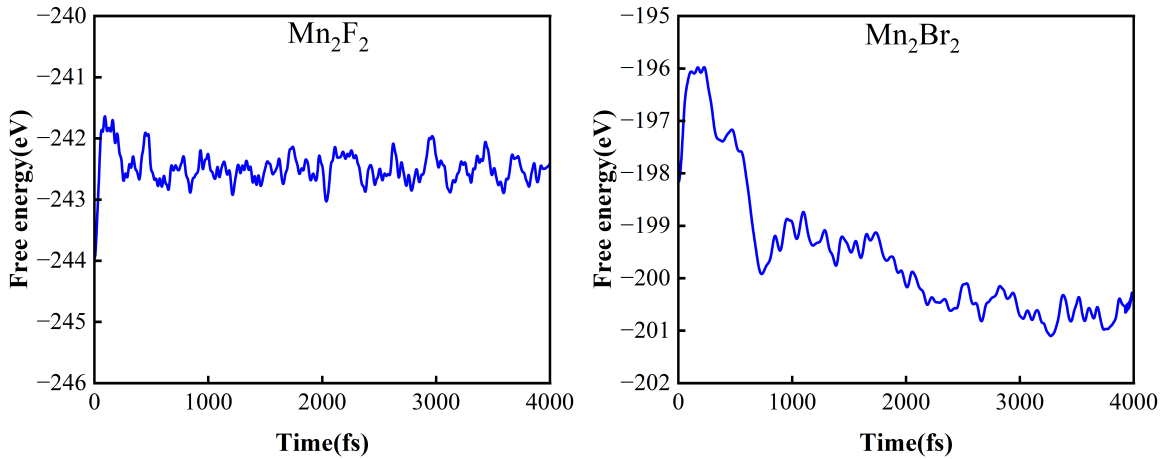


FIG. S2: AIMD simulations of Mn₂Br₂ and Mn₂F₂.

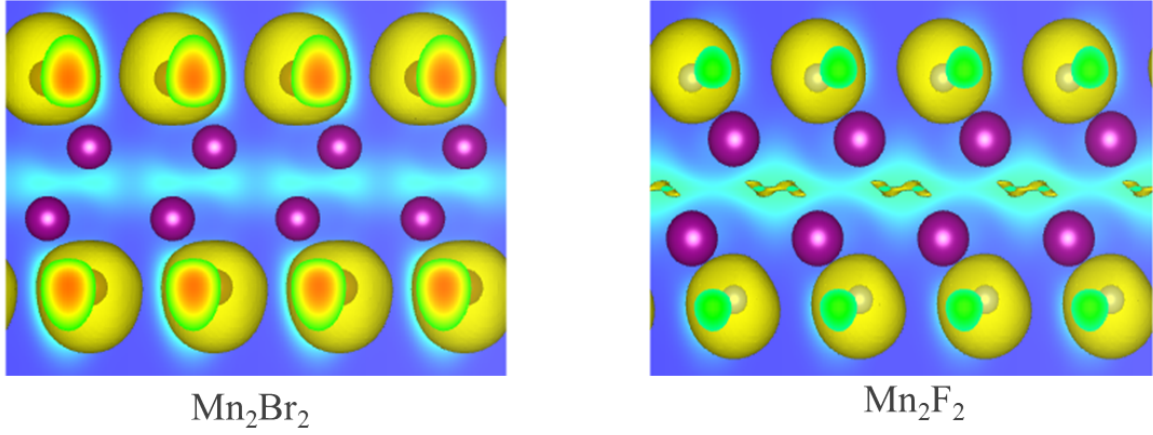


FIG. S3: ELF of Mn_2Br_2 and Mn_2F_2 .

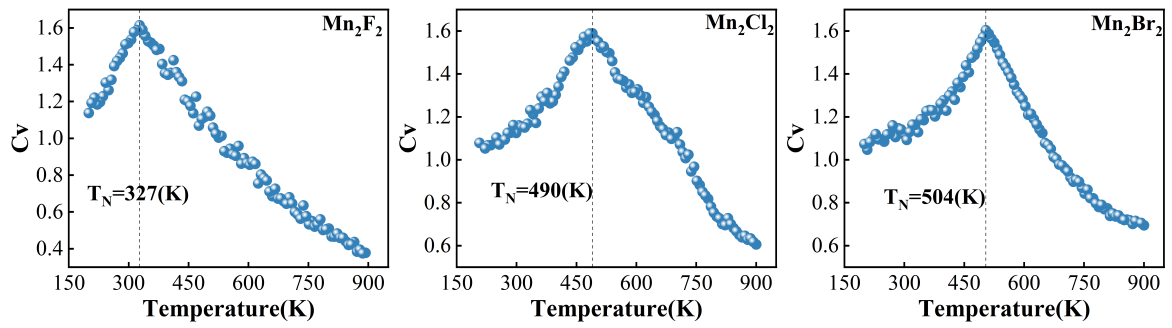


FIG. S4: T_N of monolayer Mn_2X_2 .

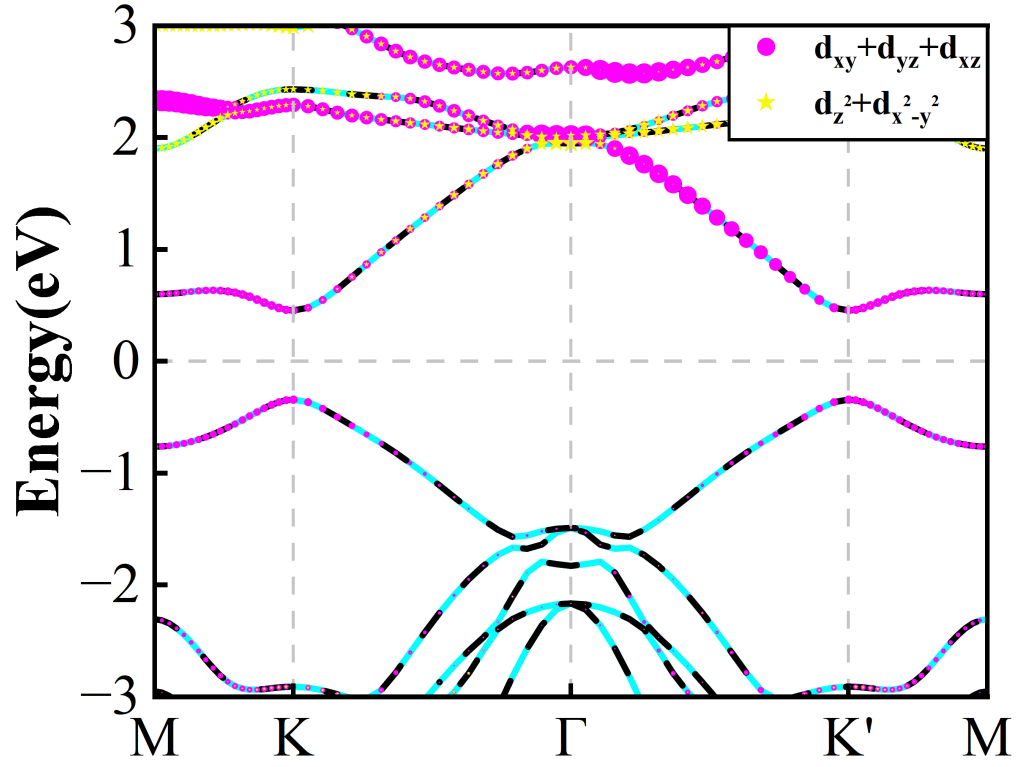


FIG. S5: PBAND of monolayer Mn_2Br_2 without SOC.

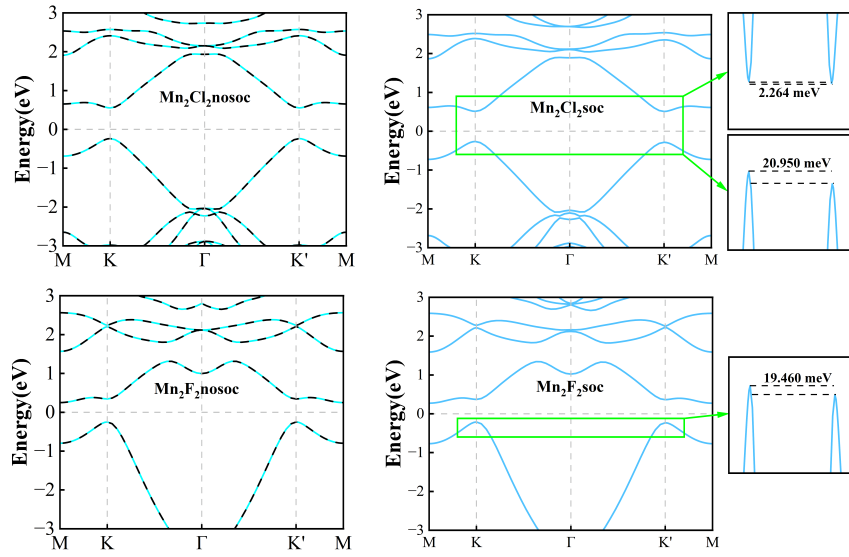


FIG. S6: Band structures of Mn_2Cl_2 and Mn_2F_2 with and without SOC.

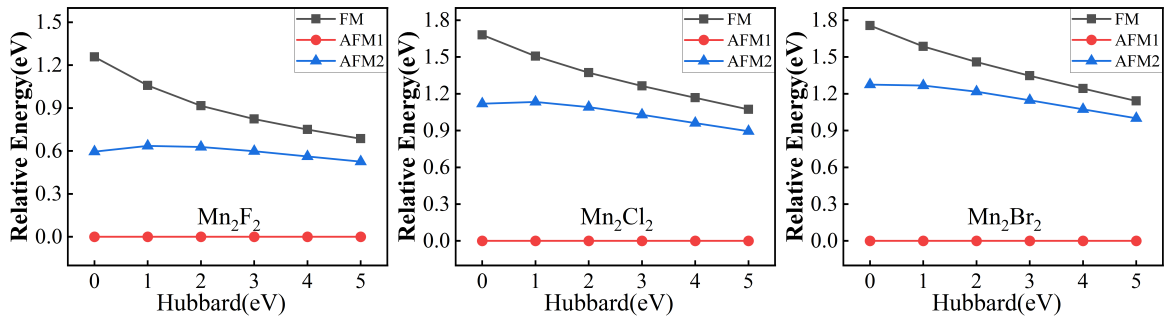
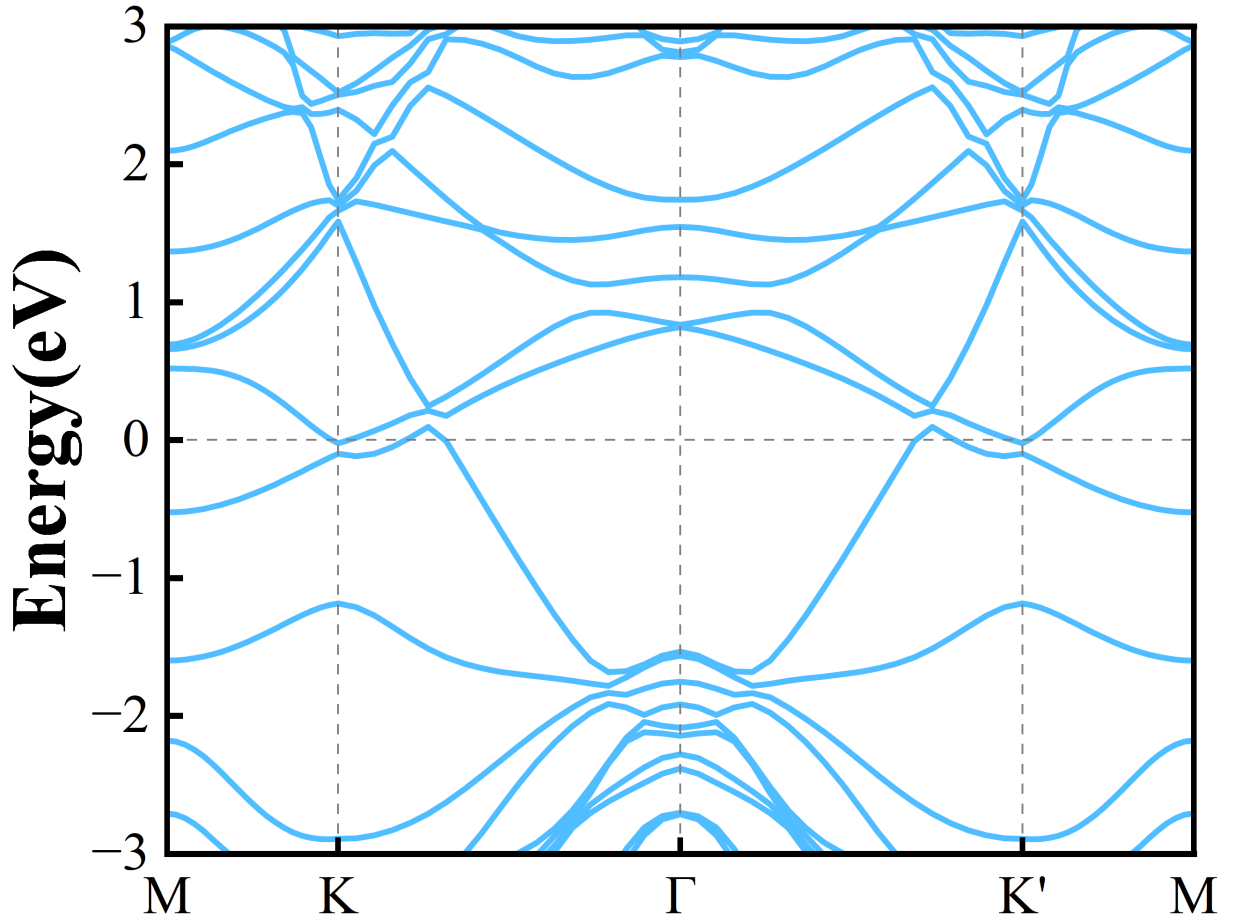


FIG. S8: Total energies of monolayer Mn_2X_2 for different magnetic configurations as a function of the Hubbard U , with the energies measured relative to the AFM1 state.

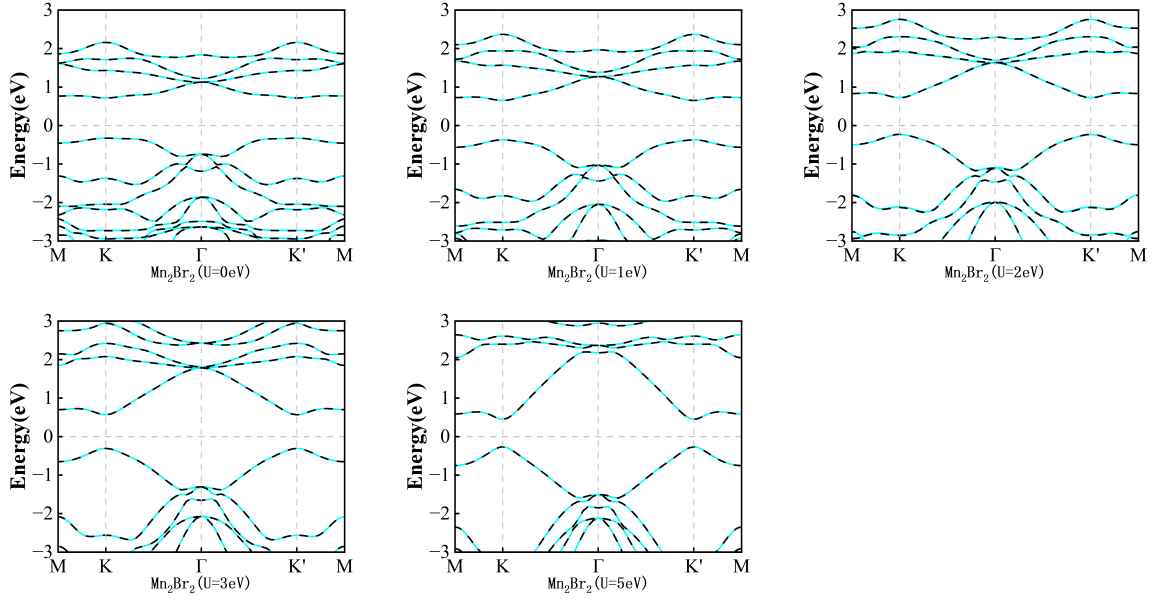


FIG. S9: Band structures of Mn_2Br_2 without SOC under different Hubbard U values.

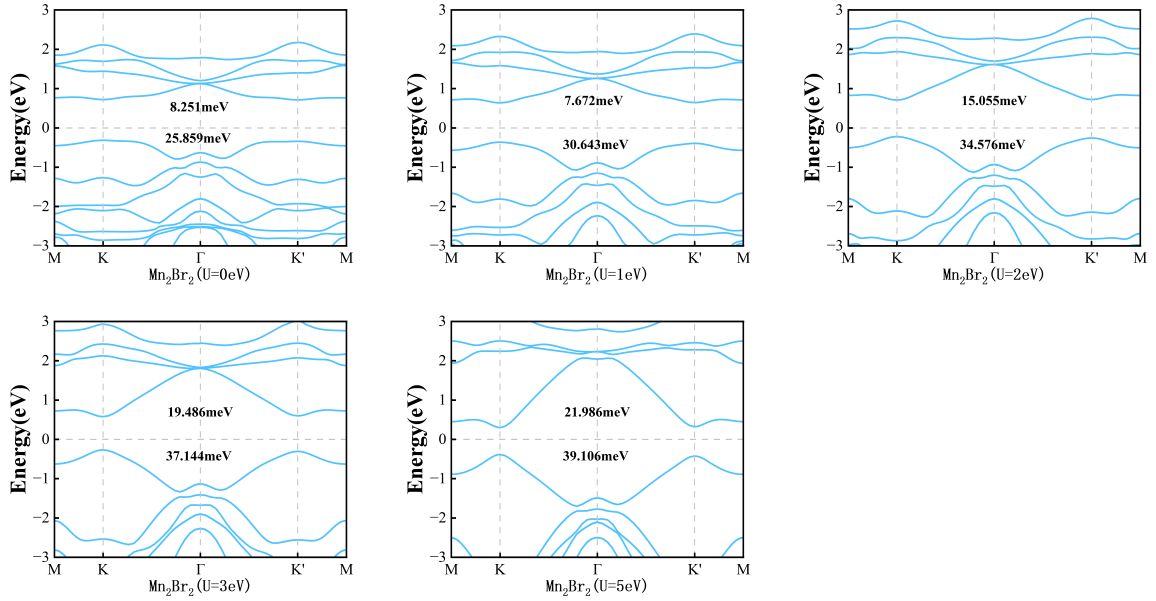


FIG. S10: Band structures of Mn_2Br_2 with SOC under different Hubbard U values.

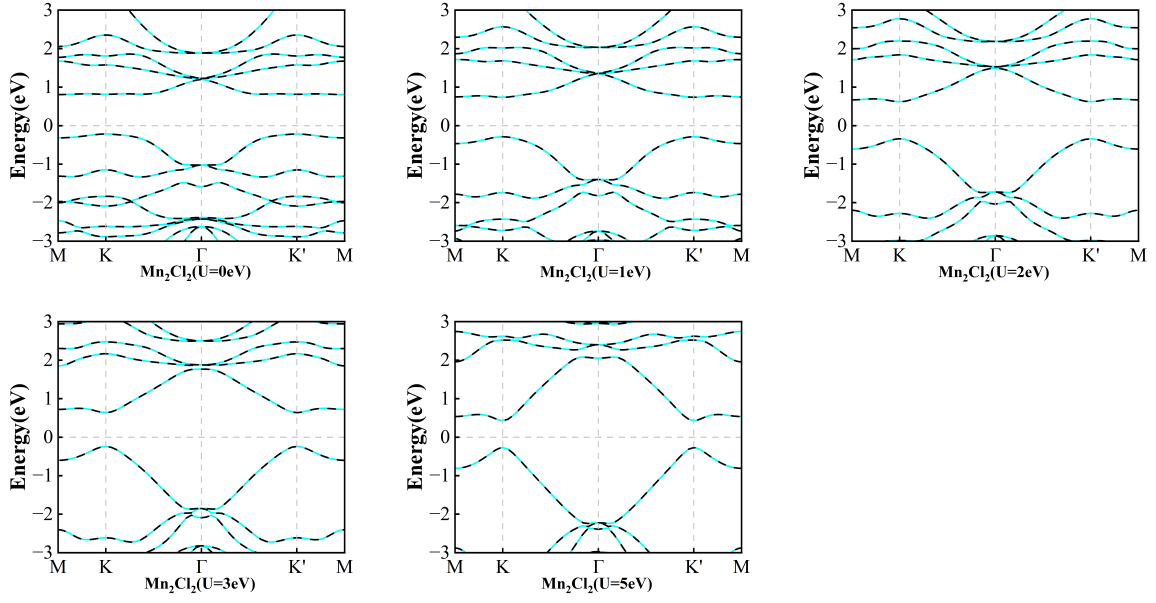


FIG. S11: Band structures of Mn_2Cl_2 without SOC under different Hubbard U values.

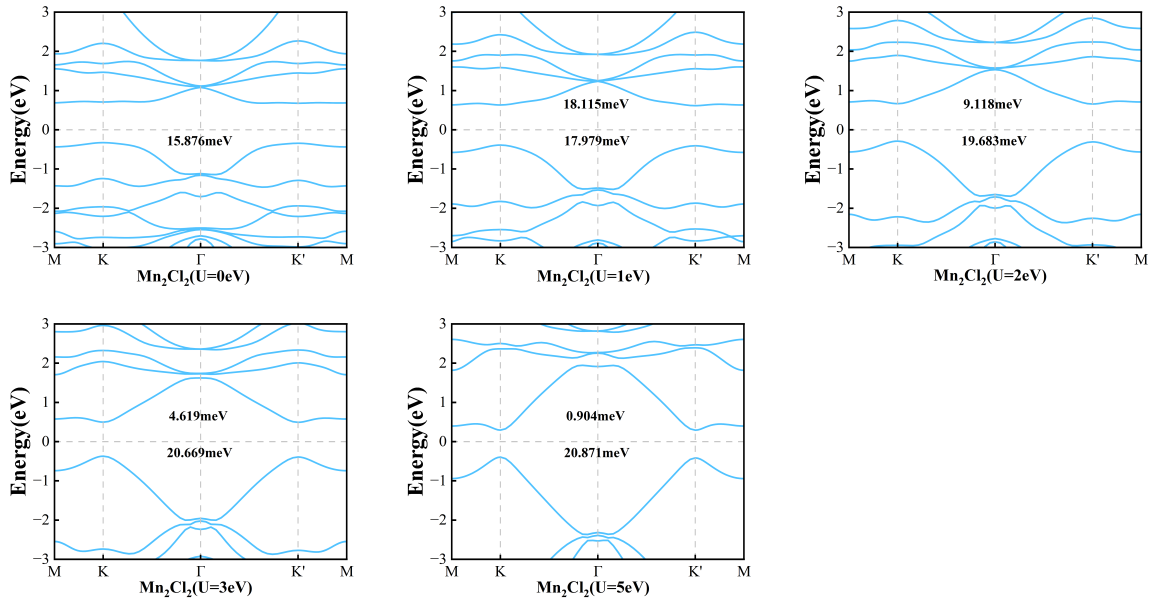


FIG. S12: Band structures of Mn_2Cl_2 with SOC under different Hubbard U values.

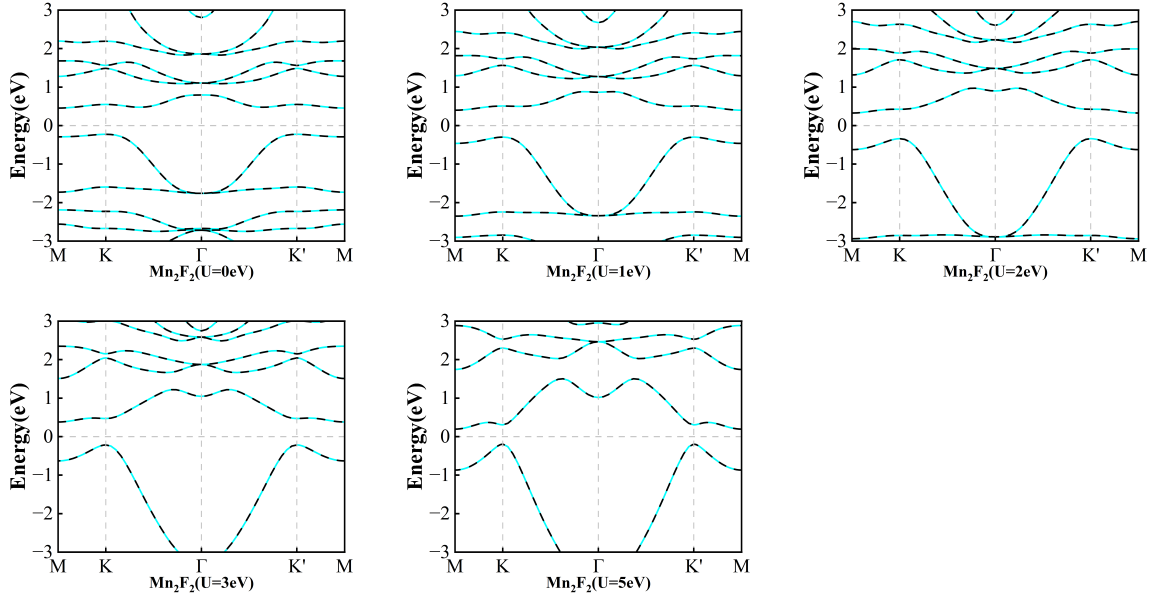


FIG. S13: Band structures of Mn_2F_2 without SOC under different Hubbard U values.

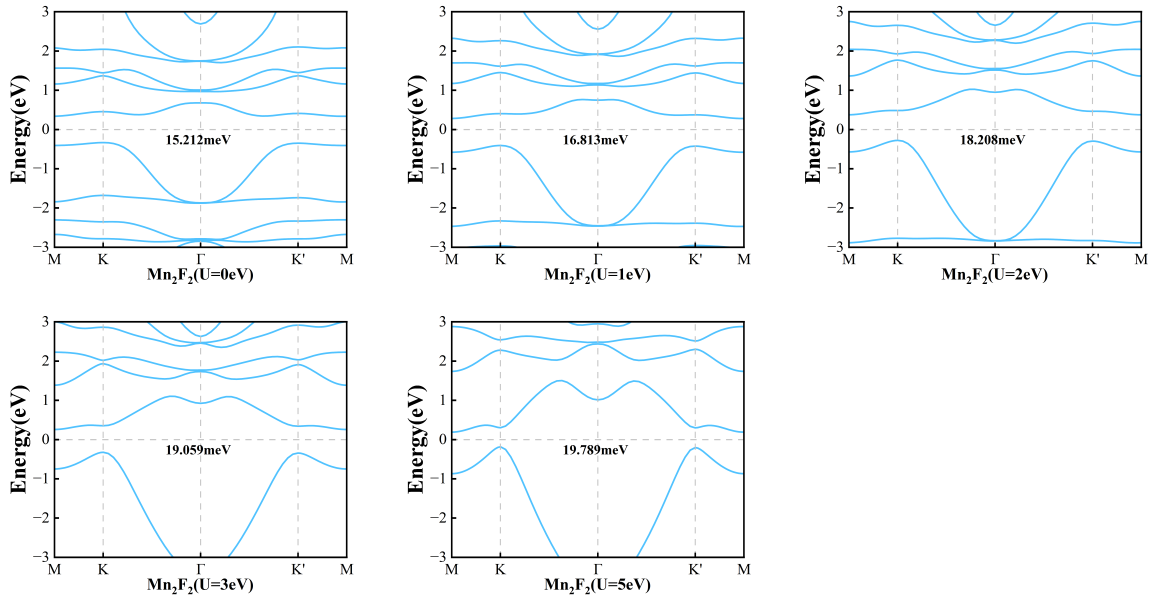


FIG. S14: Band structures of Mn_2F_2 with SOC under different Hubbard U values.

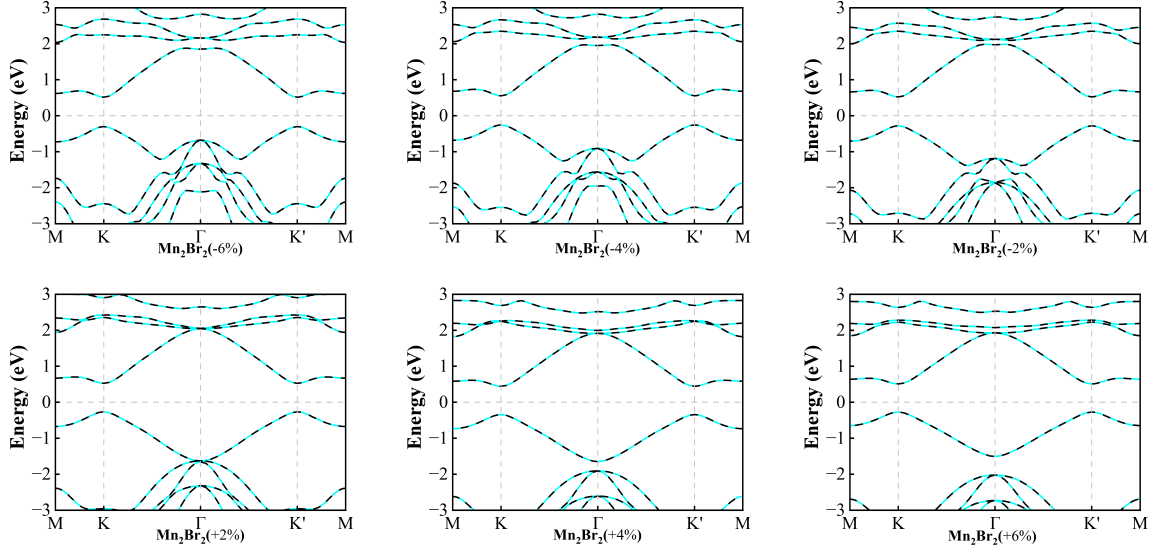


FIG. S15: Band structures of Mn_2Br_2 without SOC under different strain values.

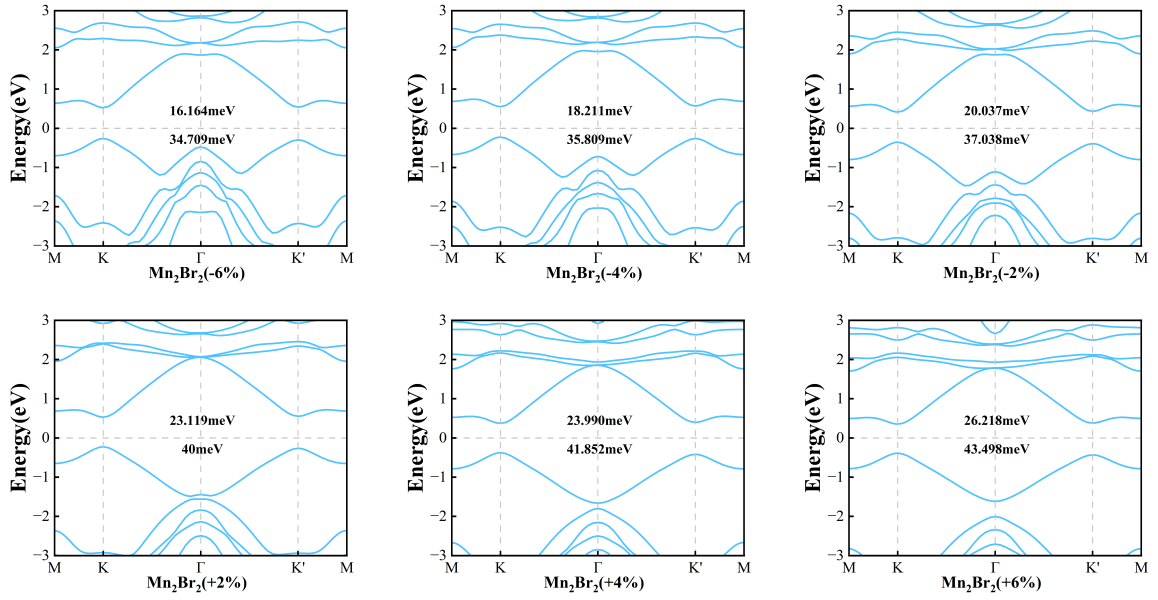


FIG. S16: Band structures of Mn_2Br_2 with SOC under different strain values.

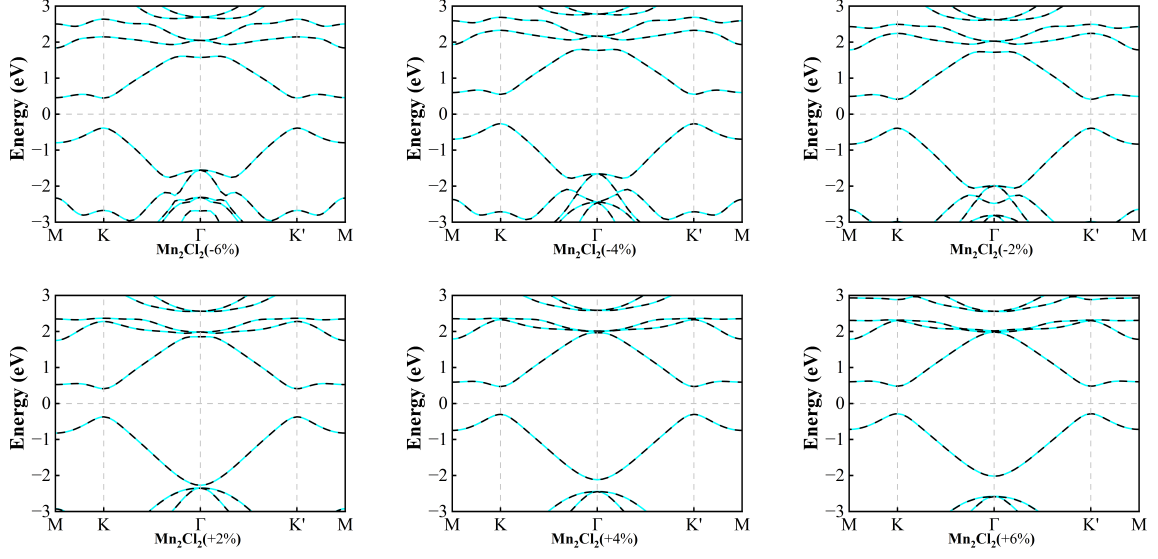


FIG. S17: Band structures of Mn_2Cl_2 without SOC under different strain values.

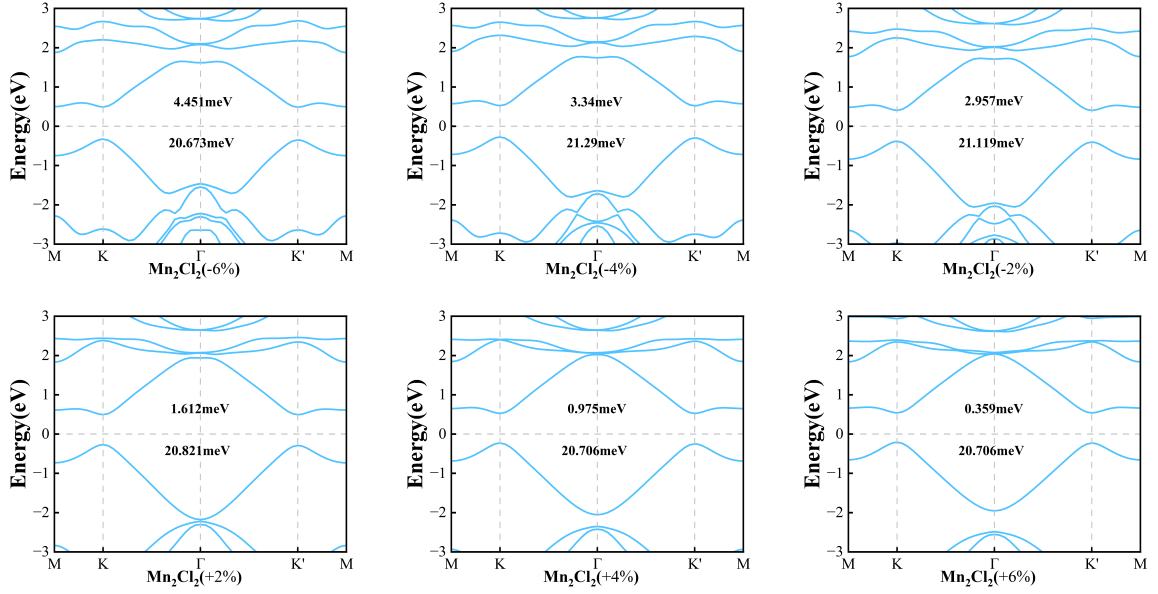


FIG. S18: Band structures of Mn_2Cl_2 with SOC under different strain values.

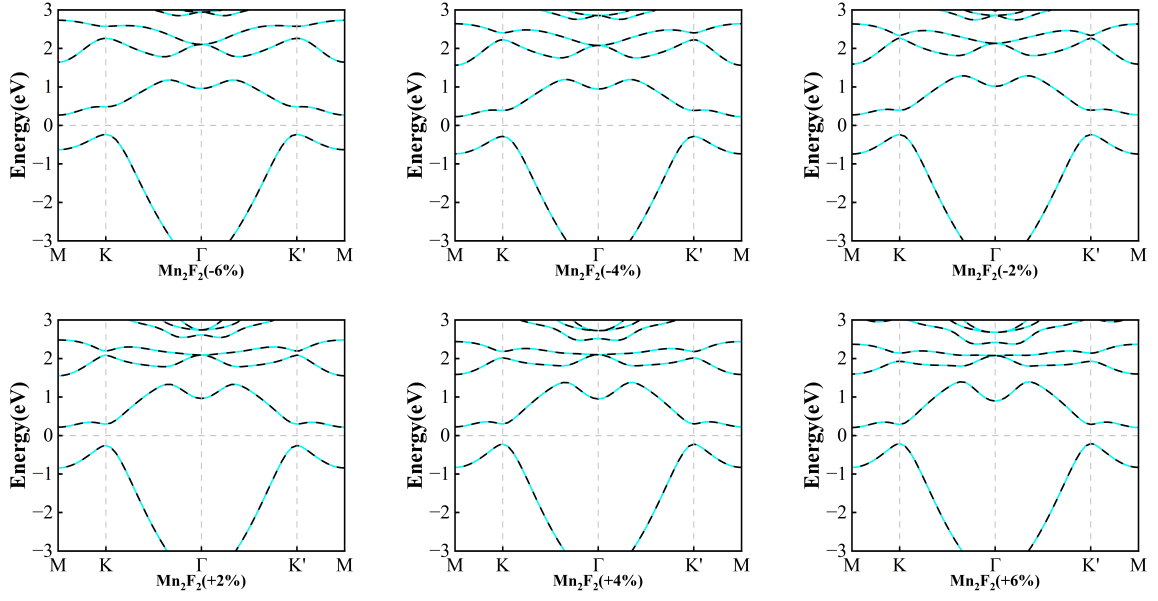


FIG. S19: Band structures of Mn_2F_2 without SOC under different strain values.

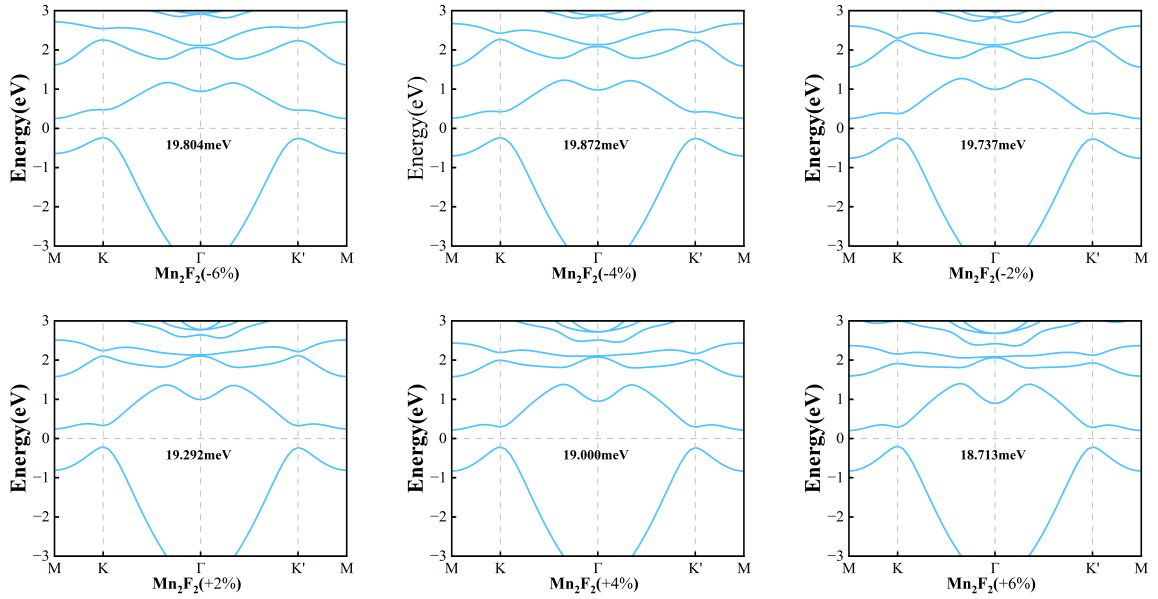


FIG. S20: Band structures of Mn_2F_2 with SOC under different strain values.

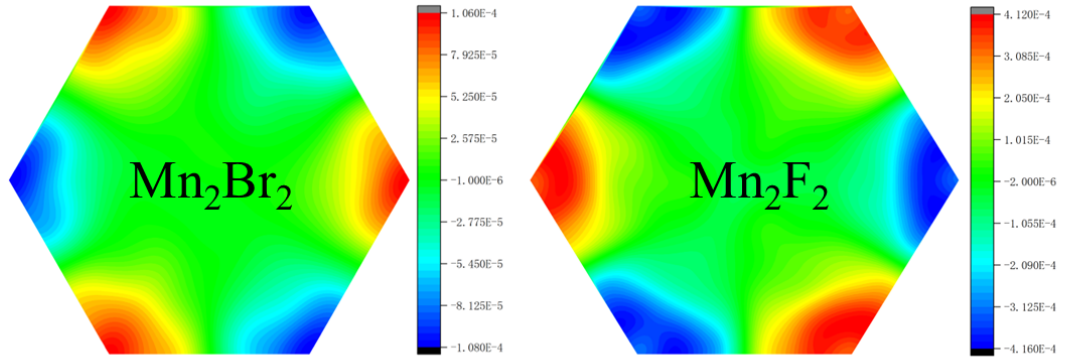


FIG. S21: Berry curvatures of monolayer Mn_2Br_2 and Mn_2F_2 .